AIAA JOURNAL
Vol. 34, No. 7, July 1996

Free Vibration of Thick Generally Laminated Cantilever Quadrilateral Plates

Rakesh K. Kapania* and Andrew E. Lovejoy†
Virginia Polytechnic Institute and State University, Blacksburg, Virginia, 24061-0203

Free vibration of plate structures of various material systems has been vastly studied. Transverse shear can play an important role even in thin laminated structures and therefore must be included in the analysis. A method applicable to the study of generally laminated, thick, skew, trapezoidal plates is developed as there appears to be limited information available in this area. Using Chebychev polynomials as displacement functions in the Rayleigh–Ritz method, the first-order shear deformation theory is utilized to account for the transverse shear effects. All appropriate inertia terms are retained. Boundary conditions are enforced by the appropriate use of distributed linear and rotational springs along the edges. Thus, the method is applicable to any supported quadrilateral plate but is applied to cantilever plates in this study. After the validity of the method is established through comparison to published results, an extensive study is made of thick, symmetrically laminated and unsymmetrically laminated, cantilever, skew, trapezoidal plates.

Introduction

THE growing use of structures fabricated from composite materials has facilitated the development of methods for the analysis of these structures. Composite laminated plates find uses in many areas, including aircraft structures. Early methods of analysis for these plates focused on the classical laminate theory (CLT),[1,2] which involves many simplifying assumptions, e.g., the neglect of transverse shear and normal stress. However, in laminated or single layer plates in which the transverse shear modulus is small compared with the extensional modulus, as well as in thick plates, transverse shear has a pronounced effect and cannot be neglected. Overestimation of the natural frequencies occurs when CLT is used for analysis. This arises from the assumption of Kirchhoff, where transverse shear stiffness is considered to be infinite. Consequently, many theories that include transverse shear have been developed and utilized by many researchers. These include, among others, the first-order shear deformation theory (FSDT),[3] a third-order shear deformation theory (TSDT),[4] which is a member of the group of higher order shear deformation theories (HSDT),[5] and layerwise theories (LWT).[6] The number of papers that study the free vibration of quadrilateral plates is quite voluminous, and an in-depth review of theories and approaches can be found in the reference by Lovejoy and Kapania,[7] as well as a number of others.[8–15] Here, a thick plate will be considered as one in which transverse shear has a significant effect and must be included in the analysis. Modern wing structures, for example, have components that can be represented as skew trapezoidal plates (nonisosceles). In spite of this, only a few works that include shear effects for these plates have been published. Because of this apparent lack of information, and also because wing panels are increasingly composed of composite materials, a need for studying these structures using a theory that incorporates transverse shear effects is recognized.

The purpose of this work is to determine the natural frequencies and mode shapes of thick, skew, trapezoidal, generally laminated, cantilever plates. Here, the Rayleigh–Ritz method, a well-known method for finding approximate solutions, is used. We take into account transverse shear using the FSDT and include rotary inertia terms. Following the earlier work of Kapania and Singhvi,[16] Chebychev polynomials are employed in this study. The essential boundary conditions are approximately satisfied by applying appropriate artificial springs to the edges, adding to the total potential energy. Choosing Chebychev polynomials and applying artificial springs allow for the analysis of arbitrarily supported plates without the need for finding functions that are dependent upon the support conditions, that is, those that satisfy the essential boundary conditions. Thus, this method provides an analysis technique for the free vibration of arbitrarily supported, thick, generally laminated, quadrilateral plates using a single set of functions.

Considering the skew, trapezoidal, isotropic, cantilever plates, a number of references are of interest.[17–21] The integral equation technique was employed to study thin, cantilever plates by Srinivasan and Babu.[17] Joshi and Madhusudhan[18] used finite elements for cantilever plates, whereas Laura et al.[19] used the Rayleigh–Ritz method with two-dimensional, orthogonal polynomials. McGee et al.[20] utilized polynomials and corner functions in the Rayleigh–Ritz method in their study. Thick, isotropic, plates were studied using an HSDT finite element by McGee and Butalia.[21] Pertaining to trapezoidal, orthotropic, or anisotropic plates, only analyses of isosceles plates are available. Liew and Lam[22] studied plates with various boundary conditions. They used the Rayleigh–Ritz method utilizing two-dimensional orthogonal polynomials.

Laminated, isosceles, trapezoid, cantilever plates were analyzed by Krishnan and Deshpande[23] by means of finite elements. Skew, trapezoidal, thin, laminated plates are treated by Kapania and Singhvi.[16] The method used in Ref. 16 is similar to the one used in this work; however, transverse shear is neglected. Finite elements, based on the FSDT, are used by both Lakshminarayana et al.[24] and Lee and Lee[25] to study skew, laminated plates, but results are presented only for thin plates. Thus, it is our intent to expand the knowledge base for the free, undamped, natural vibration of generally laminated, thick, skew, trapezoidal, cantilever plates. The present method is a simple, computationally fast method for determining the natural frequencies of any quadrilateral plate composed of any linearly elastic material system. Therefore, as with the more computationally intense finite element method, the present method removes the restrictions found in many previous methods pertaining to plate shape, such as rectangular, or plate material, such as isotropic. The plate may have edges that are combinations of clamped, simply supported, and free boundary conditions; however, cantilever plates are extensively studied using the present method.

Theory

Letting z be the transverse coordinate, to incorporate transverse shear in a plate theory, one could choose displacement functions that

Received Dec. 5, 1994; presented as Paper 95-1350 at the AIAA/ASME/ASCE/AHS/ASC 36th Structures, Structural Dynamics, and Materials Conference, New Orleans, LA, April 10–13, 1995; revision received June 1, 1995; accepted for publication Aug. 10, 1995.

*Professor, Department of Aerospace and Ocean Engineering. Associate Fellow AIAA.

†Graduate Research Assistant, Department of Aerospace and Ocean Engineering. Student Member AIAA.

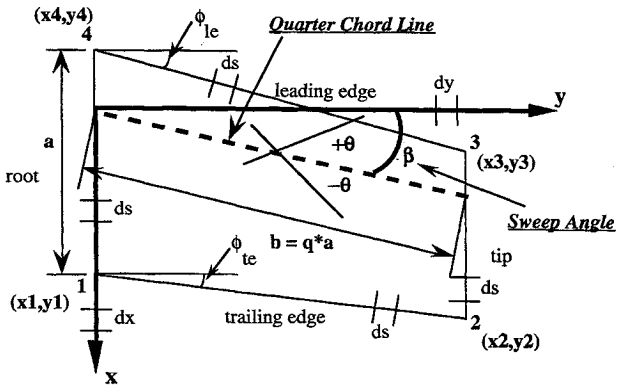

a) Original coordinates

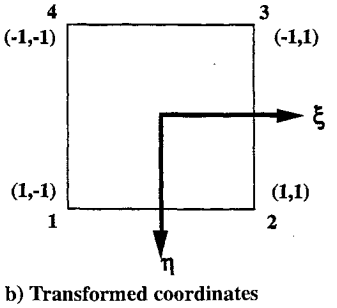

b) Transformed coordinates

Fig. 1 Plate definitions and transformed coordinates.

are linear in z, the FSDT, or displacement functions that are higher order functions of z, an HSDT. In the present study, the simplest of these relations, the FSDT, is chosen. Consider FSDT with the following displacement functions[3]:

$$u = u^0(x, y, t) + z\phi_x(x, y, t)$$
$$v = v^0(x, y, t) + z\phi_y(x, y, t); \qquad w = w^0(x, y, t) \tag{1}$$

where u, v, and w are the displacements in the x, y, and z directions, respectively. The superscript 0 denotes that the quantity is associated with the midplane. Midplane displacements, u^0 and v^0, are included to allow the study of unsymmetric laminates.

The domain is transformed to make the integrals computationally simple and to facilitate the use of Chebychev polynomials as trial displacement functions when expanding the displacements of Eq. (1). The choice of the Chebychev polynomials is made for several reasons. First, these polynomials allow for ease of integration through Gauss quadrature and can lead to analytical sensitivity calculations of the stiffness and mass matrices. Second, since the essential boundary conditions are enforced through the application of artificial springs rather than satisfied explicitly, the same set of deflection can be used for any type of supported plate. Lastly, the orthogonality property of the Chebychev polynomials is expected to allow for a larger number of terms in the series before numerical ill-conditioning arises, as is the case with regular polynomials. The skew trapezoidal plate is transformed into a square region with vertices having values ranging from -1 to 1 as seen in Fig. 1. The familiar related transformation equations for this mapping are given by

$$x = \sum_{i=1}^{4} N_i(\eta, \xi)x_i; \qquad y = \sum_{i=1}^{4} N_i(\eta, \xi)y_i \tag{2}$$

where

$$N_1 = \tfrac{1}{4}(1+\eta)(1-\xi); \qquad N_2 = \tfrac{1}{4}(1+\eta)(1+\xi)$$
$$N_3 = \tfrac{1}{4}(1-\eta)(1+\xi); \qquad N_4 = \tfrac{1}{4}(1-\eta)(1-\xi) \tag{3}$$

and x_i and y_i are the corner coordinates of the plate defined in Fig. 1. Taking the derivatives of the Cartesian coordinates x and y in terms of the transformed coordinates η and ξ, the Jacobian for the transformation can easily be determined.

Now, Chebyshev polynomials that are functions of the transformed coordinates η and ξ are taken to be the trial displacement functions for the Rayleigh–Ritz method:

$$u^0 = \sum_{i=0}^{I}\sum_{j=0}^{J} R_{ij}(t)T_i(\eta)T_j(\xi)$$
$$v^0 = \sum_{k=0}^{K}\sum_{l=0}^{L} S_{kl}(t)T_k(\eta)T_l(\xi)$$
$$w^0 = \sum_{m=0}^{M}\sum_{n=0}^{N} P_{mn}(t)T_m(\eta)T_n(\xi) \tag{4}$$
$$\phi_x = \sum_{p=0}^{P}\sum_{q=0}^{Q} X_{pq}(t)T_p(\eta)T_q(\xi)$$
$$\phi_y = \sum_{r=0}^{R}\sum_{s=0}^{S} Y_{rs}(t)T_r(\eta)T_s(\xi)$$

where R_{ij}, S_{kl}, P_{mn}, X_{pq}, and Y_{rs} are the time-dependent Rayleigh–Ritz coefficients. The recursive formula for the Chebychev polynomials is given by

$$T_0(\Psi) = 1; \qquad T_1(\Psi) = \Psi$$
$$T_i(\Psi) = 2\Psi T_{i-1}(\Psi) - T_{i-2}(\Psi); \qquad -1 \le \Psi \le 1 \tag{5}$$

To find the natural frequencies for the plate, we solve an eigenvalue problem of the form

$$[K - \lambda M]\{q\} = 0 \tag{6}$$

$$\{q\} = \{R_{00}, R_{01}, \ldots, R_{IJ}, S_{00}, \ldots, S_{KL}, X_{00}, \ldots, X_{PQ},$$
$$Y_{00}, \ldots, Y_{RS}, P_{00}, \ldots, P_{MN}\}^T \tag{7}$$

The total stiffness matrix is found to be $K = K_{\text{strain}} + K_{\text{springs}}$, the summation of the stiffness matrices associated with the strain energy and boundary spring approximations. To construct the stiffness and mass matrices, K and M, respectively, Lagrange's equations are utilized.

The kinetic energy of the plate is calculated, recognizing that for laminated composite plates it is possible that each lamina may have a different functional value for ρ_k, the volume mass density for the kth layer. Using the deflection functions of Eq. (1), performing some mathematical manipulation, and integrating through the plate thickness h result in the following:

$$T = \frac{1}{2}\int\int_A \left\{\rho_1\left[\left(\frac{\partial u^0}{\partial t}\right)^2 + \left(\frac{\partial v^0}{\partial t}\right)^2 + \left(\frac{\partial w^0}{\partial t}\right)^2\right]\right.$$
$$+ 2\rho_2\left[\left(\frac{\partial u^0}{\partial t}\right)\left(\frac{\partial \phi_x}{\partial t}\right) + \left(\frac{\partial v^0}{\partial t}\right)\left(\frac{\partial \phi_y}{\partial t}\right)\right]$$
$$\left. + \rho_3\left[\left(\frac{\partial \phi_x}{\partial t}\right)^2 + \left(\frac{\partial \phi_y}{\partial t}\right)^2\right]\right\} dx\, dy \tag{8}$$

where we define

$$\rho_1 = \int_{-\frac{h}{2}}^{\frac{h}{2}} \rho_k\, dz; \qquad \rho_2 = \int_{-\frac{h}{2}}^{\frac{h}{2}} \rho_k z\, dz; \qquad \rho_3 = \int_{-\frac{h}{2}}^{\frac{h}{2}} \rho_k z^2\, dz \tag{9}$$

Note that if the laminate is density symmetric about the midplane, $\rho_2 = 0$. After substitution the mass matrix can then be written as

$$M = \int_{-1}^{1}\int_{-1}^{1} \{[Z]^T[\rho_\Psi][Z]\}|J|\, d\eta\, d\xi \tag{10}$$

where

$$[Z] = \left[\begin{array}{c|c|c|c|c} \{T_{\mu v}\} & 0 & 0 & 0 & 0 \\ \hline 0 & \{T_{\mu v}\} & 0 & 0 & 0 \\ \hline 0 & 0 & \{T_{\mu v}\} & 0 & 0 \\ \hline 0 & 0 & 0 & \{T_{\mu v}\} & 0 \\ \hline 0 & 0 & 0 & 0 & \{T_{\mu v}\} \end{array}\right] \tag{11}$$

$$[\rho_\Psi] = \begin{bmatrix} \rho_1 & 0 & \rho_2 & 0 & 0 \\ 0 & \rho_1 & 0 & \rho_2 & 0 \\ \rho_2 & 0 & \rho_3 & 0 & 0 \\ 0 & \rho_2 & 0 & \rho_3 & 0 \\ 0 & 0 & 0 & 0 & \rho_1 \end{bmatrix} \tag{12}$$

an expression for the strain energy in terms of the strains and the laminate stiffnesses, A_{ij}, B_{ij}, and D_{ij}.

The strain energy integral is transformed, as was the kinetic energy integral, to use the natural coordinates η and ξ. First, the strains are transformed by means of the chain rule, and substitution with algebraic manipulation results in the following for the stiffness matrix:

$$K_{\text{Strain}} = \int_{-1}^{1}\int_{-1}^{1} [C]^T[T]^T \left[\begin{array}{c|c|c} A & B & \\ \hline B & D & 0 \\ \hline & 0 & A' \end{array}\right] [T][C]|J|\,d\eta\,d\xi \tag{14}$$

where

$$[T] = \begin{bmatrix} (J_{12}^T)^{-1} & (J_{11}^T)^{-1} & 0 & 0 & 0 & 0 & 0 & 0 & 0 & 0 & 0 & 0 \\ 0 & 0 & (J_{22}^T)^{-1} & (J_{21}^T)^{-1} & 0 & 0 & 0 & 0 & 0 & 0 & 0 & 0 \\ (J_{22}^T)^{-1} & (J_{21}^T)^{-1} & (J_{12}^T)^{-1} & (J_{11}^T)^{-1} & 0 & 0 & 0 & 0 & 0 & 0 & 0 & 0 \\ 0 & 0 & 0 & 0 & (J_{12}^T)^{-1} & (J_{11}^T)^{-1} & 0 & 0 & 0 & 0 & 0 & 0 \\ 0 & 0 & 0 & 0 & 0 & 0 & (J_{22}^T)^{-1} & (J_{21}^T)^{-1} & 0 & 0 & 0 & 0 \\ 0 & 0 & 0 & 0 & (J_{22}^T)^{-1} & (J_{21}^T)^{-1} & (J_{12}^T)^{-1} & (J_{11}^T)^{-1} & 0 & 0 & 0 & 0 \\ 0 & 0 & 0 & 0 & 0 & 0 & 0 & 0 & (J_{22}^T)^{-1} & (J_{21}^T)^{-1} & 1 & 0 \\ 0 & 0 & 0 & 0 & 0 & 0 & 0 & 0 & (J_{12}^T)^{-1} & (J_{11}^T)^{-1} & 0 & 1 \end{bmatrix} \tag{15}$$

$$[C] = \begin{bmatrix} [T_{\mu v,\zeta}] & 0 & 0 & 0 & 0 \\ 0 & [T_{\mu v,\zeta}] & 0 & 0 & 0 \\ 0 & 0 & [T_{\mu v,\zeta}] & 0 & 0 \\ 0 & 0 & 0 & [T_{\mu v,\zeta}] & 0 \\ 0 & 0 & 0 & 0 & [T_{\mu v,\zeta}] \\ 0 & 0 & 0 & \{T_{\mu v}\} & 0 \\ 0 & 0 & \{T_{\mu v}\} & 0 & 0 \end{bmatrix} \tag{16}$$

and

$$[T_{\mu v,\zeta}] = \begin{bmatrix} T_0(\eta)\dfrac{\partial T_0(\xi)}{\partial \xi} & T_0(\eta)\dfrac{\partial T_1(\xi)}{\partial \xi} & T_0(\eta)\dfrac{\partial T_2(\xi)}{\partial \xi} & \cdots & T_\mu(\eta)\dfrac{\partial T_v(\xi)}{\partial \xi} \\ T_0(\xi)\dfrac{\partial T_0(\eta)}{\partial \eta} & T_1(\xi)\dfrac{\partial T_0(\eta)}{\partial \eta} & T_2(\xi)\dfrac{\partial T_0(\eta)}{\partial \eta} & \cdots & T_v(\xi)\dfrac{\partial T_\mu(\eta)}{\partial \eta} \end{bmatrix} \tag{17}$$

and

$$\{T_{\mu v}\} = \{T_0(\eta)T_0(\xi), T_0(\eta)T_1(\xi), T_0(\eta)T_2(\xi), \ldots, T_\mu(\eta)T_v(\xi)\} \tag{13}$$

In Eq. (10), $|J|$ is the determinant of the Jacobian matrix. The subscript pairs are $\mu v = IJ, KL, PQ, RS$, and MN and we restrict $I = K = P = R = M$ and $J = L = Q = S = N$ to facilitate programming. The various 0 in the preceding relations are appropriately sized matrices whose components are all zero.

In a manner consistent with Cook et al.,[26] a matrix form of the strain energy can be developed that involves the stiffness matrix. To calculate the stiffness matrix in the present method, the constitutive relation from Cederbaum et al.[27] is utilized. When the transverse stress is zero, $\sigma_z = 0$, the stresses are related to the strains only through the reduced stiffnesses. These reduced stiffnesses are then transformed in accordance to the lamina orientation in a generally laminated plate as discussed by Jones[1] and Vinson and Sierakowski.[2] Substituting for the stress vectors in the strain energy equation and then integrating through the thickness lead to

$$K_{\text{strain}} = \int_{-1}^{1}\int_{-1}^{1} [C]^T[T]^T \left[\begin{array}{c|c|c} A & B & \\ \hline B & D & 0 \\ \hline & 0 & A' \end{array}\right] [T][C]|J|\,d\eta\,d\xi \tag{14}$$

where

$$[T] = \begin{bmatrix} (J_{12}^T)^{-1} & (J_{11}^T)^{-1} & 0 & 0 & 0 & 0 & 0 & 0 & 0 & 0 & 0 & 0 \\ 0 & 0 & (J_{22}^T)^{-1} & (J_{21}^T)^{-1} & 0 & 0 & 0 & 0 & 0 & 0 & 0 & 0 \\ (J_{22}^T)^{-1} & (J_{21}^T)^{-1} & (J_{12}^T)^{-1} & (J_{11}^T)^{-1} & 0 & 0 & 0 & 0 & 0 & 0 & 0 & 0 \\ 0 & 0 & 0 & 0 & (J_{12}^T)^{-1} & (J_{11}^T)^{-1} & 0 & 0 & 0 & 0 & 0 & 0 \\ 0 & 0 & 0 & 0 & 0 & 0 & (J_{22}^T)^{-1} & (J_{21}^T)^{-1} & 0 & 0 & 0 & 0 \\ 0 & 0 & 0 & 0 & (J_{22}^T)^{-1} & (J_{21}^T)^{-1} & (J_{12}^T)^{-1} & (J_{11}^T)^{-1} & 0 & 0 & 0 & 0 \\ 0 & 0 & 0 & 0 & 0 & 0 & 0 & 0 & (J_{22}^T)^{-1} & (J_{21}^T)^{-1} & 1 & 0 \\ 0 & 0 & 0 & 0 & 0 & 0 & 0 & 0 & (J_{12}^T)^{-1} & (J_{11}^T)^{-1} & 0 & 1 \end{bmatrix} \tag{15}$$

$$[C] = \begin{bmatrix} [T_{\mu v,\zeta}] & 0 & 0 & 0 & 0 \\ 0 & [T_{\mu v,\zeta}] & 0 & 0 & 0 \\ 0 & 0 & [T_{\mu v,\zeta}] & 0 & 0 \\ 0 & 0 & 0 & [T_{\mu v,\zeta}] & 0 \\ 0 & 0 & 0 & 0 & [T_{\mu v,\zeta}] \\ 0 & 0 & 0 & \{T_{\mu v}\} & 0 \\ 0 & 0 & \{T_{\mu v}\} & 0 & 0 \end{bmatrix} \tag{16}$$

and

$$[T_{\mu v,\zeta}] = \begin{bmatrix} T_0(\eta)\dfrac{\partial T_0(\xi)}{\partial \xi} & T_0(\eta)\dfrac{\partial T_1(\xi)}{\partial \xi} & T_0(\eta)\dfrac{\partial T_2(\xi)}{\partial \xi} & \cdots & T_\mu(\eta)\dfrac{\partial T_v(\xi)}{\partial \xi} \\ T_0(\xi)\dfrac{\partial T_0(\eta)}{\partial \eta} & T_1(\xi)\dfrac{\partial T_0(\eta)}{\partial \eta} & T_2(\xi)\dfrac{\partial T_0(\eta)}{\partial \eta} & \cdots & T_v(\xi)\dfrac{\partial T_\mu(\eta)}{\partial \eta} \end{bmatrix} \tag{17}$$

and $\{T_{\mu v}\}$ is given in Eq. (13). Components in the matrix represented by Eq. (15) are components in the inverse of the transpose of the Jacobian matrix. The subscript pairs μv and the various 0 in the preceding matrices are as discussed for the mass matrix. The terms A, B, and D in Eq. (14) are the CLT laminate stiffness matrices, and the A' matrix represents the contribution from including transverse shear and is given by

$$A' = \begin{bmatrix} k_4^2 A_{44} & k_4 k_5 A_{45} \\ k_4 k_5 A_{45} & k_5^2 A_{55} \end{bmatrix} \tag{18}$$

In the present method, the values $k_4 = k_5 = \sqrt{(\pi^2/12)}$ are chosen for the laminate shear correction factors in accordance with Mindlin,[28] which is appropriate for comparative purposes with the references. They could also be found from stacking sequence dependent integral forms as has been done by several authors.[29–35]

Using the formulations for K_{strain} and M, the free vibration analysis of completely free plates can be performed. This is done to validate the development of these two matrices, and analysis has

been carried out with comparison made to a number of published results.[7] For brevity, results for these plates are omitted here, but mention should be made that the results showed excellent agreement. Now, to consider generally supported plates, the essential boundary conditions must be satisfied. These boundary conditions for the plate are modeled by introducing appropriate linear and rotational springs, which prevent the linear and rotational motion along the boundary, respectively. The spring terms contribute to the potential energy of the plate, V, and thus are needed for their contribution to the Lagrangian when applying Hamilton's principle, which will yield the total stiffness and mass matrices.

Consider two types of simply supported edges, namely, SS1, $u^0 = v^0 = w^0 = 0$, and SS2, $u^0 = w^0 = \phi_y = 0$ or $v^0 = w^0 = \phi_x = 0$. The essential boundary conditions for a simply supported laminated plate using the FSDT are given by Reddy and Chao[36] as the SS2 type. For a clamped edge, the boundary conditions are given as $u^0 = v^0 = w^0 = \phi_x = \phi_y = 0$. Let the spring constraints be represented by α_ζ and β_ζ for the linear and rotational springs, respectively. Subscripts appended to the spring terms will represent the root r, the tip t, the leading edge le, and the trailing edge te. The expressions for the strain energy for the springs that are approximating the essential boundary conditions along the root are given as

$$\frac{1}{2}\int_{x_1}^{x_4} \alpha_{r_x}(u^0)^2 ds; \qquad \frac{1}{2}\int_{x_1}^{x_4} \alpha_{r_y}(v^0)^2 ds$$

$$\frac{1}{2}\int_{x_1}^{x_4} \alpha_{r_z}(w^0)^2 ds; \qquad \frac{1}{2}\int_{x_1}^{x_4} \beta_{r_x}(\phi_y)^2 ds \tag{19}$$

$$\frac{1}{2}\int_{x_1}^{x_4} \beta_{r_y}(\phi_x)^2 ds$$

where ds is an infinitesimal increment along the edge. Similar equations apply to the remaining edges. The second subscript in the linear spring constant terms denotes the direction of the displacement, and that in the rotational spring constant terms represents the axis about which the moment is taken. Relationships for ds along any edge in terms of dx and dy are easily developed, and complete details are given in Ref. 7. The integrals from Eq. (19) are evaluated where required by the boundary conditions, resulting in

$$K_{\text{springs}} = \int_{-1}^{1} \begin{bmatrix} K_{11} & 0 & 0 & 0 & 0 \\ 0 & K_{22} & 0 & 0 & 0 \\ 0 & 0 & K_{33} & 0 & 0 \\ 0 & 0 & 0 & K_{44} & 0 \\ 0 & 0 & 0 & 0 & K_{55} \end{bmatrix} d\gamma \tag{20}$$

where

$$\begin{aligned}
K_{11} &= \tilde{\alpha}_{t_x}[T_{\mu\nu\mu\nu}]_t + \tilde{\alpha}_{te_x}[T_{\mu\nu\mu\nu}]_{te} + \tilde{\alpha}_{r_x}[T_{\mu\nu\mu\nu}]_r \\
&\quad + \tilde{\alpha}_{le_x}[T_{\mu\nu\mu\nu}]_{le} \\
K_{22} &= \tilde{\alpha}_{t_y}[T_{\mu\nu\mu\nu}]_t + \tilde{\alpha}_{te_y}[T_{\mu\nu\mu\nu}]_{te} + \tilde{\alpha}_{r_y}[T_{\mu\nu\mu\nu}]_r \\
&\quad + \tilde{\alpha}_{le_y}[T_{\mu\nu\mu\nu}]_{le} \\
K_{33} &= \tilde{\beta}_{r_y}[T_{\mu\nu\mu\nu}]_t + \tilde{\beta}_{te_y}[T_{\mu\nu\mu\nu}]_{te} + \tilde{\beta}_{r_y}[T_{\mu\nu\mu\nu}]_r \\
&\quad + \tilde{\beta}_{le_y}[T_{\mu\nu\mu\nu}]_{le} \\
K_{44} &= \tilde{\beta}_{t_x}[T_{\mu\nu\mu\nu}]_t + \tilde{\beta}_{te_x}[T_{\mu\nu\mu\nu}]_{te} + \tilde{\beta}_{r_x}[T_{\mu\nu\mu\nu}]_r \\
&\quad + \tilde{\beta}_{le_x}[T_{\mu\nu\mu\nu}]_{le} \\
K_{55} &= \tilde{\alpha}_{t_z}[T_{\mu\nu\mu\nu}]_t + \tilde{\alpha}_{te_z}[T_{\mu\nu\mu\nu}]_{te} + \tilde{\alpha}_{r_z}[T_{\mu\nu\mu\nu}]_r \\
&\quad + \tilde{\alpha}_{le_z}[T_{\mu\nu\mu\nu}]_{le}
\end{aligned} \tag{21}$$

where

$$\begin{aligned}
[T_{\mu\nu\mu\nu}]_r &= \{T_{\mu\nu}\}_r{}^T\{T_{\mu\nu}\}_r; \qquad [T_{\mu\nu\mu\nu}]_t = \{T_{\mu\nu}\}_t{}^T\{T_{\mu\nu}\}_t \\
[T_{\mu\nu\mu\nu}]_{le} &= \{T_{\mu\nu}\}_{le}{}^T\{T_{\mu\nu}\}_{le}; \qquad [T_{\mu\nu\mu\nu}]_{te} = \{T_{\mu\nu}\}_{te}{}^T\{T_{\mu\nu}\}_{te}
\end{aligned} \tag{22}$$

Table 1 Frequency parameter, $\Omega = \omega(a\cos\gamma)^2\sqrt{(\rho h/D)}$, for the first five frequencies of a thick, isotropic, skew, cantilever, trapezoidal plate, $\gamma = 45$ deg, $b/h = 5$, and $\nu = 0.3$

a/b	c/b	McGree and Butalia[21,a]	Present study[b]
	0.25	1.8736	1.8711
		2.7500*	2.7601**
		4.4483	4.4320
		6.1457*	6.2140**
		6.6329	6.6663
0.5	0.5	1.8796	1.8743
		3.0799*	3.0918**
		3.7052	3.7303
		6.2646	5.9907**
		6.7578	6.7687
	1.0	1.8977	1.8903
		3.1280	3.1109
		3.2321*	3.2448**
		4.3257	4.6021
		4.6365	5.7267**
	0.25	2.1388	2.1422
		4.0566*	4.0659**
		7.8998	7.8876
		10.6325	10.6446
		12.0308*	12.0664**
1.0	0.5	1.9318	2.0527
		5.1316*	4.4904**
		5.9034	6.6110
		9.7586	10.4775
		12.7414*	12.3079**
	1.0	2.0944	2.0930
		4.7789	4.7793
		5.4330*	5.4371**
		10.4651	10.4264
		11.8488	11.7548**
	0.25	2.2870	2.2944
		5.2498*	5.2625**
		10.5004	10.5256
		18.0996	18.1676
		18.5316*	18.5376**
2.0	0.5	2.0772	2.0814
		5.4399*	5.4476**
		10.1204	10.1290
		14.5838	14.8340
		21.3361*	21.3544**
	1.0	1.9803	1.9822
		6.2778*	6.2817**
		8.0619	8.0740
		12.8975	12.9221
		21.9190	21.9115

[a] In-plane modes indicated by *.
[b] In-plane modes indicated by **.

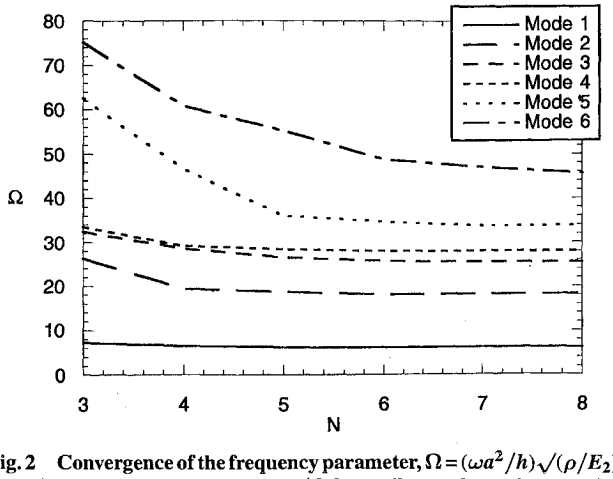

Fig. 2 Convergence of the frequency parameter, $\Omega = (\omega a^2/h)\sqrt{(\rho/E_2)}$, for thick, laminated, skew, trapezoidal, cantilever plate with stacking sequence $[-30/30/0]_s$, $\beta = -45$ deg, and taper ratio = 0.25.

Table 2 Three lowest frequencies, in hertz, of a thin, laminated $[\theta_2/0]_s$, cantilever plate with $\beta = 30$ deg, thickness = 3.556 mm (0.14 in.), area = 406.45 cm^2 (63.0 in.^{2}), aspect ratio = 3.111, and taper ratio = 0.5 and made of glass/epoxy

Stacking sequence	Mode no.	Lee and Lee[25]	Lakshminarayana et al.[24,a]	Lakshminarayana et al.[24,b]	Kapania and Singhvi[16]	Present study
$[0_2/0]_s$	1	16.80	16.67	17.55	17.30	17.25
	2	81.03	80.40	83.80	84.44	83.77
	3	100.08	99.52	98.65	98.29	97.70
$[15_2/0]_s$	1	16.00	15.90	15.70	16.96	16.91
	2	75.08	73.50	73.60	77.28	76.73
	3	111.98	114.56	108.15	111.40	110.62
$[30_2/0]_s$	1	13.18	13.15	13.90	13.94	13.91
	2	67.61	66.67	65.70	69.65	69.30
	3	116.65	120.86	110.80	116.59	115.55
$[45_2/0]_s$	1	10.45	11.05	11.05	11.48	11.47
	2	59.01	59.13	57.01	60.13	59.97
	3	112.55	117.37	116.10	114.46	113.38
$[60_2/0]_s$	1	9.33	9.82	10.10	10.04	10.04
	2	52.98	53.5	52.75	53.48	53.38
	3	100.65	105.6	105.25	103.36	102.52
$[75_2/0]_s$	1	9.24	9.16	9.60	9.31	9.30
	2	52.98	49.84	50.30	49.78	49.63
	3	88.99	93.38	91.35	90.79	90.24
$[90_2/0]_s$	1	8.60	8.82	8.45	9.00	8.98
	2	47.43	47.41	45.45	48.01	47.82
	3	82.64	86.58	89.15	83.25	82.79

[a]Calculated. [b]Experimental.

Table 3 Five lowest frequencies, in hertz, of a thin, symmetrically laminated $[30_2/0]_s$, cantilever plate with thickness = 3.556 mm (0.14 in.), area = 406.45 cm^2 (63.0 in^2), and taper ratio = 0.5 and made of glass/epoxy

	$AR = 1.0$		$AR = 3.111$		$AR = 5.0$	
β, deg	Kapania and Singhvi[16]	Present study	Kapania and Singhvi[16]	Present study	Kapania and Singhvi[16]	Present study
−45	24.55	24.45	7.42	7.40	4.55	4.54
	102.55	101.81	40.17	40.01	24.77	24.72
	156.13	155.14	103.51	102.19	66.57	66.29
	255.23	253.15	109.78	109.21	102.24	100.34
	408.53	408.07	209.03	222.64	130.17	114.48
−30	34.37	34.25	10.98	10.94	6.78	6.76
	123.02	122.10	59.48	59.21	36.88	36.74
	189.31	188.28	106.43	104.92	99.29	98.80
	322.66	319.88	160.59	159.76	103.07	101.28
	434.13	430.60	270.80	266.62	194.01	202.03
−15	44.13	43.99	14.01	13.96	8.60	8.57
	130.55	129.69	75.76	75.41	46.70	46.51
	235.46	234.26	107.98	106.59	103.69	101.97
	360.12	357.33	204.80	203.69	126.15	125.53
	398.32	394.90	280.28	276.23	245.96	255.50
0	53.36	53.22	16.01	15.95	9.62	9.58
	131.41	130.63	83.23	82.79	51.89	51.66
	281.33	279.83	113.05	111.84	104.67	103.17
	356.54	354.16	221.29	219.84	139.85	139.14
	408.59	405.17	300.27	297.25	260.66	260.22
15	59.42	59.29	16.19	16.14	9.44	9.42
	129.29	128.58	80.38	79.93	50.55	50.34
	296.06	294.36	118.34	117.25	105.21	103.86
	357.68	355.59	210.12	208.71	135.89	135.48
	437.44	433.94	314.71	313.69	252.11	257.94
30	58.86	58.75	13.94	13.91	7.89	7.90
	122.64	121.99	69.65	69.30	42.35	42.29
	284.42	282.72	116.59	115.55	103.06	101.61
	353.91	352.04	181.59	181.13	115.60	116.36
	462.66	458.82	294.88	298.11	216.28	227.72
45	47.30	47.21	9.52	9.54	5.33	5.37
	108.78	108.17	49.83	49.82	28.87	29.07
	259.31	257.77	109.00	107.93	76.79	78.42
	299.90	298.41	133.54	136.18	104.11	103.50
	433.82	434.79	239.86	250.46	152.34	130.54

Table 4 Five lowest frequencies, in hertz, of a thin, unsymmetrically laminated [0/22.5], cantilever plate with thickness = 1.2497 mm (0.0492 in.), area = 412.9 cm^2 (64.0 in^2), and taper ratio = 0.75 and made of boron/epoxy

	$AR = 1.0$		$AR = 3.111$		$AR = 5.0$	
β, deg	Kapania and Singhvi[16]	Present study	Kapania and Singhvi[16]	Present study	Kapania and Singhvi[16]	Present study
−45	18.19	16.70	5.84	5.40	3.46	3.22
	54.24	50.40	33.98	31.38	20.34	18.91
	107.47	99.84	45.28	43.21	43.06	41.10
	152.15	140.24	93.16	85.93	55.95	51.95
	234.14	214.34	128.74	122.23	109.53	109.22
−30	26.77	24.51	8.75	8.06	5.19	4.81
	60.28	56.47	46.28	43.81	30.56	28.32
	149.09	137.10	51.36	47.40	43.67	41.49
	170.77	155.37	135.58	126.61	84.31	78.02
	220.05	202.58	142.00	131.65	123.47	116.65
−15	33.91	30.85	11.08	10.18	6.55	6.05
	64.65	60.06	46.84	44.47	37.73	35.20
	151.71	138.63	44.13	60.44	45.19	42.53
	202.45	184.11	141.15	133.00	104.39	97.07
	241.28	221.87	183.04	167.30	129.72	121.42
0	38.03	34.70	12.26	11.26	7.18	6.63
	67.20	62.23	46.38	44.06	38.99	36.77
	145.42	133.52	74.53	68.27	48.20	44.86
	227.30	207.22	140.61	132.22	108.20	101.48
	260.77	237.97	208.14	190.39	138.88	128.90
15	38.28	35.18	11.92	10.96	6.88	6.36
	66.64	61.67	44.61	42.39	36.63	34.49
	142.16	130.93	74.81	68.58	48.94	45.67
	231.09	212.61	132.06	124.09	100.54	94.32
	263.26	239.88	210.92	193.27	141.46	131.87
30	34.18	31.23	9.99	9.20	5.67	5.25
	61.82	57.44	41.11	39.04	31.07	29.05
	141.53	130.02	66.34	61.21	46.87	44.30
	210.35	191.63	115.84	108.99	84.15	78.70
	252.34	230.43	190.18	175.33	134.27	126.59
45	25.41	23.22	6.82	6.33	3.82	3.57
	53.06	49.76	33.95	31.91	21.79	20.35
	138.39	126.98	53.05	49.94	44.27	42.29
	161.55	147.83	90.90	85.33	59.15	55.37
	241.51	221.81	151.87	143.91	113.75	114.37

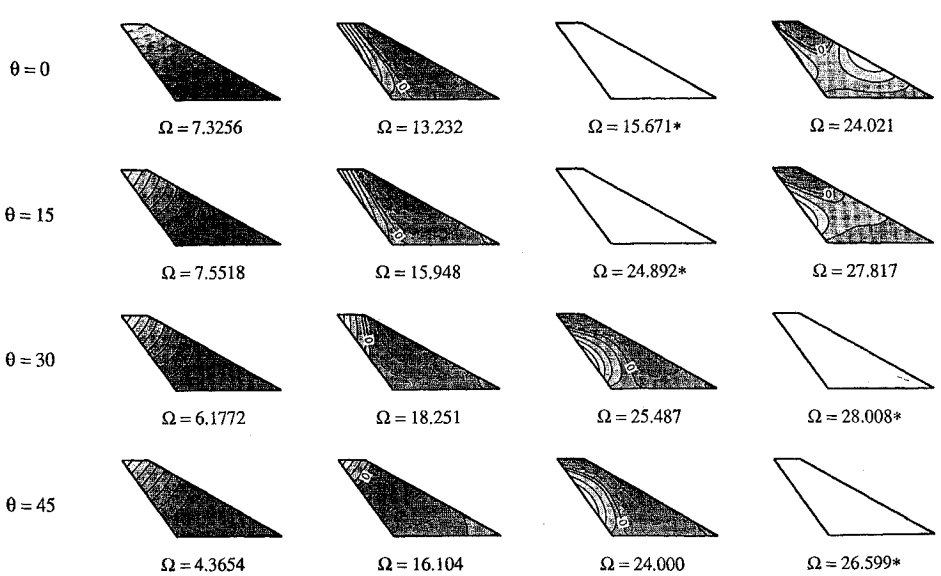

Fig. 3 Frequency parameters and mode shapes of cantilever, thick, skew, trapezoidal, symmetrically laminated $[-\theta/\theta/0]_s$ plates, $\Omega = (\omega a^2/h)\sqrt{(\rho/E_2)}$, $\beta = -45$ deg, $q = 1.0$, $a/h = 10$, taper ratio = 0.25 (*in-plane mode).

Table 5 Frequency parameter, $\Omega = (\omega a^2/h)\sqrt{(\rho/E_2)}$, for the first four frequencies of a cantilever, symmetrically laminated $[0_3]$s, thick, skew, trapezoidal plate, with length-to-thickness ratio $a/h = 10$

q	Taper ratio	Sweep angle β, deg −45	−30	0	30	45
	0.25	7.33	7.06	6.85	7.01	7.41
		13.2	12.3	11.9	13.8	16.7
		15.7*	15.1*	14.9*	17.3*	19.9*
		24.0	22.9	22.5	23.5	24.8
1.00	0.50	6.56	6.35	6.20	6.33	6.65
		10.0	9.30	9.05	10.4	12.2
		14.5*	13.8*	13.5*	15.2*	17.1*
		21.8	20.0	18.7	21.3	23.4
	1.00	5.78	5.65	5.58	5.65	5.78
		6.87	6.37	6.10	6.37	6.87
		13.3*	11.0	9.53	11.0	13.3*
		13.5	12.4*	11.6*	12.4*	13.5
	0.25	2.11	2.07	2.05	2.10	2.20
		5.41	5.00	4.93	5.77	6.75
		6.70*	6.93*	7.14*	7.63*	7.88*
		9.17	8.89	8.67	8.79	9.12
2.00	0.50	1.84	1.82	1.80	1.84	1.91
		4.01	3.65	3.53	4.03	4.62
		6.19*	6.31*	6.41*	6.74*	6.89*
		8.68	8.46	8.32	8.47	8.77
	1.00	1.58	1.56	1.55	1.56	1.58
		2.53	2.26	2.10	2.26	2.53
		5.62*	5.59*	5.46*	5.59*	5.62*
		8.33	7.90	6.93	7.90	8.33
	0.25	0.361	0.360	0.361	0.371	0.382
		1.59	1.50	1.46	1.67	1.79
		1.76*	1.82*	1.75	1.76	1.94
		1.97	2.03	2.24*	2.14*	1.94
5.00	0.50	0.309	0.307	0.308	0.315	0.321
		1.27	1.13	1.05	1.18	1.36
		1.64	1.65	1.63	1.65	1.70
		1.69	1.85*	2.03*	1.92*	1.74*
	1.00	0.259	0.257	0.255	0.257	0.259
		0.788	0.681	0.614	0.681	0.788
		1.50*	1.55	1.54	1.55	1.50*
		1.58	1.65*	1.73*	1.65*	1.58

*In-plane mode.

Table 6 Frequency parameter, $\Omega = (\omega a^2/h)\sqrt{(\rho/E_2)}$, for the first frequencies of a cantilever, symmetrically laminated $[-30/30/0]_s$, thick, skew, trapezoidal plate, with length-to-thickness ratio $a/h = 10$

q	Taper ratio	Sweep angle β, deg −45	−30	0	30	45
	0.25	6.18	5.73	5.21	5.90	7.24
		18.3	16.6	16.4	17.2	18.4
		25.5	22.9	19.5	22.6	28.2
		28.0*	31.5	32.4	36.1*	36.5*
1.00	0.50	5.57	5.14	4.59	5.04	5.96
		14.8	13.3	12.7	13.2	14.1
		23.4	20.9	18.3	21.2	25.8
		26.2*	27.0	27.1	30.9	31.7*
	1.00	4.92	4.58	4.01	4.03	4.35
		10.7	9.07	8.21	8.72	9.66
		19.7	16.4	14.2	16.4	19.6
		20.5	19.8	19.4	20.8	22.7
	0.25	1.41	1.38	1.34	1.45	1.61
		6.08	5.89	5.85	6.24	6.74
		8.31*	9.36	8.24	9.09	10.5
		10.7	10.0*	12.1*	12.3*	11.5*
2.00	0.50	1.25	1.22	1.16	1.21	1.31
		5.76	5.53	5.58	5.58	5.85
		7.96*	7.34	6.19	7.15	8.44
		8.51	9.36*	10.9*	10.7*	9.80*
	1.00	1.15	1.09	0.987	0.973	1.01
		4.55	4.09	3.85	4.02	4.28
		6.89	6.18	5.35	5.67	6.43
		7.85*	8.76*	9.49*	8.76*	7.86*
	0.25	0.201	0.201	0.201	0.206	0.212
		0.969	0.963	0.957	0.985	1.02
		1.50*	1.84*	2.18*	2.03*	1.74*
		2.49	2.46	2.46	2.52	2.59
5.00	0.50	0.173	0.173	0.170	0.172	0.176
		0.930	0.924	0.910	0.922	0.943
		1.41*	1.71*	1.98*	1.83*	1.57*
		2.48	2.46	2.39	2.46	2.50
	1.00	0.150	0.148	0.143	0.140	0.141
		0.908	0.900	0.877	0.860	0.862
		1.37*	1.62	1.47	1.61	1.37*
		2.00	1.69	1.78*	1.65	1.94

*In-plane mode.

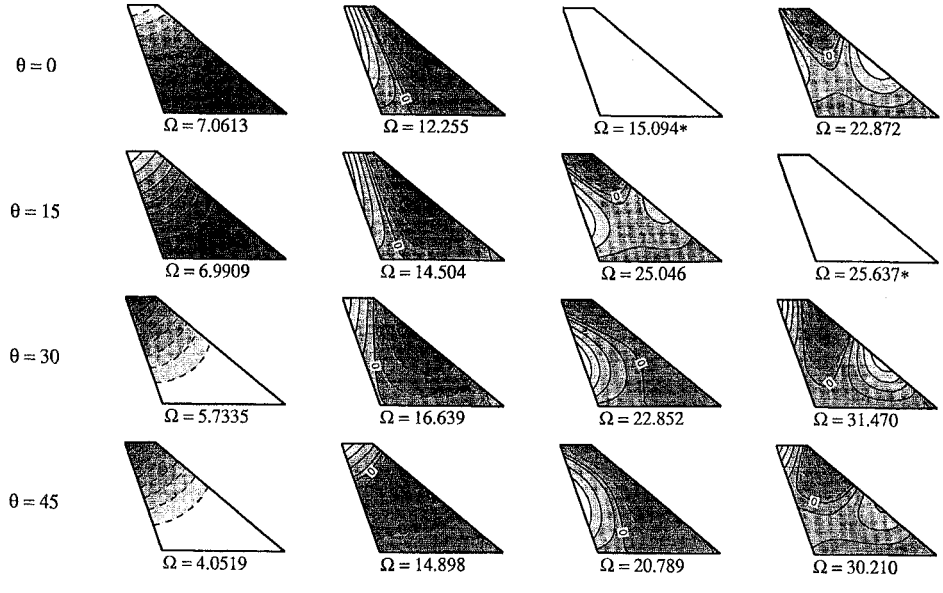

Fig. 4 Frequency parameters and mode shapes of cantilever, thick, skew, trapezoidal, symmetrically laminated $[-\theta/\theta/0]_s$ plates, $\Omega = (\omega a^2/h)\sqrt{(\rho/E_2)}$, $\beta = -30$ deg, $q = 1.0$, $a/h = 10$, taper ratio = 0.25 (*in-plane mode).

Table 7 Frequency parameter, $\Omega = (\omega a^2/h)\sqrt{(\rho/E_2)}$, for the first four frequencies of a cantilever, symmetrically laminated $[-45/45/0]_s$, thick, skew, trapezoidal plate, with length-to-thickness ratio $a/h = 10$

q	Taper ratio	Sweep angle β, deg −45	−30	0	30	45
	0.25	4.37	4.05	3.70	4.81	6.40
		16.1	14.9	14.9	15.5	17.1
		24.0	20.8	17.3	21.8	28.0
		26.6*	30.2	32.8	33.3	35.4
1.00	0.50	3.98	3.65	3.20	3.91	4.89
		14.3	13.1	13.2	12.3	13.3
		20.5	17.7	14.3	19.2	23.9
		25.7*	26.6	29.2	28.6	30.1
	1.00	3.62	3.33	2.75	2.92	3.22
		11.0	9.28	8.45	8.43	9.41
		16.8	15.6	13.1	15.4	16.9
		22.7	19.8	20.1	22.9	24.4*
	0.25	0.932	0.911	0.885	1.01	1.15
		4.29	4.14	4.04	4.56	5.12
		7.49*	8.97*	8.65	9.27	10.4
		10.4	9.66	10.0	11.3*	10.6*
2.00	0.50	0.828	0.801	0.755	0.833	0.921
		4.16	4.02	3.86	4.13	4.49
		7.26*	7.54	6.50	7.30	8.51
		8.92	8.47*	9.87*	9.84*	9.12*
	1.00	0.766	0.725	0.640	0.657	0.696
		3.85	3.72	3.72	3.41	3.50
		6.37	5.22	4.08	5.05	6.05
		7.41*	8.16*	8.73*	8.17*	7.41*
	0.25	0.131	0.130	0.128	0.134	0.140
		0.638	0.629	0.621	0.652	0.682
		1.34*	1.63	1.61	1.69	1.55*
		1.69	1.64	1.92*	1.80*	1.77
5.00	0.50	0.112	0.111	0.108	0.112	0.116
		0.612	0.602	0.588	0.607	0.629
		1.27*	1.52*	1.60	1.63*	1.39*
		1.68	1.63	1.75*	1.64	1.70
	1.00	0.0970	0.0948	0.0901	0.0904	0.0924
		0.599	0.590	0.566	0.564	0.571
		1.24*	1.44*	1.57	1.44*	1.24*
		1.67	1.65	1.58	1.60	1.61

*In-plane mode.

Table 8 Frequency parameter, $\Omega = (\omega a^2/h)\sqrt{(\rho/E_2)}$, for the first four frequencies of a cantilever, unsymmetrically laminated $[-30/30]$, thick, skew, trapezoidal plate, with length-to-thickness ratio $a/h = 10$

q	Taper ratio	Sweep angle β, deg −45	−30	0	30	45
	0.25	4.08	3.72	3.58	4.54	5.78
		13.2	12.3	12.5	13.1	14.4
		19.3	17.2	14.8	19.0	24.4
		21.0	25.3	26.8	28.1	27.1
1.00	0.50	3.64	3.28	3.10	3.80	4.67
		10.5	9.65	9.37	9.78	10.8
		17.8	15.8	14.0	17.7	22.0
		19.8	21.8	22.1	24.1	23.4
	1.00	3.23	2.91	2.62	2.91	3.23
		7.13	6.24	5.83	6.24	7.13
		15.7	13.0	11.3	13.0	15.7
		15.9	15.4	14.4	15.4	15.9
	0.25	0.961	0.925	0.925	1.08	1.23
		4.29	4.15	4.25	4.72	5.19
		5.35	6.64	5.89	6.74	7.70
		7.69	6.72	8.56	8.70	8.23
2.00	0.50	0.842	0.802	0.785	0.889	0.990
		4.00	3.85	4.03	4.08	4.39
		5.25	5.19	4.35	5.38	6.45
		6.10	6.36	7.75	7.52	6.77
	1.00	0.748	0.698	0.652	0.698	0.748
		3.05	2.77	2.64	2.77	3.05
		4.94	4.31	3.79	4.31	4.94
		5.45	6.20	6.86	6.20	5.45
	0.25	0.146	0.144	0.145	0.154	0.162
		0.705	0.693	0.696	0.743	0.780
		1.16	1.35	1.52	1.47	1.28
		1.80	1.77	1.79	1.89	1.99
5.00	0.50	0.125	0.122	0.122	0.128	0.134
		0.672	0.659	0.656	0.690	0.718
		1.09	1.28	1.39	1.33	1.19
		1.78	1.74	1.64	1.81	1.90
	1.00	0.106	0.103	0.100	0.103	0.106
		0.642	0.630	0.620	0.630	0.642
		0.910	1.12	0.984	1.12	0.912
		1.36	1.14	1.22	1.14	1.36

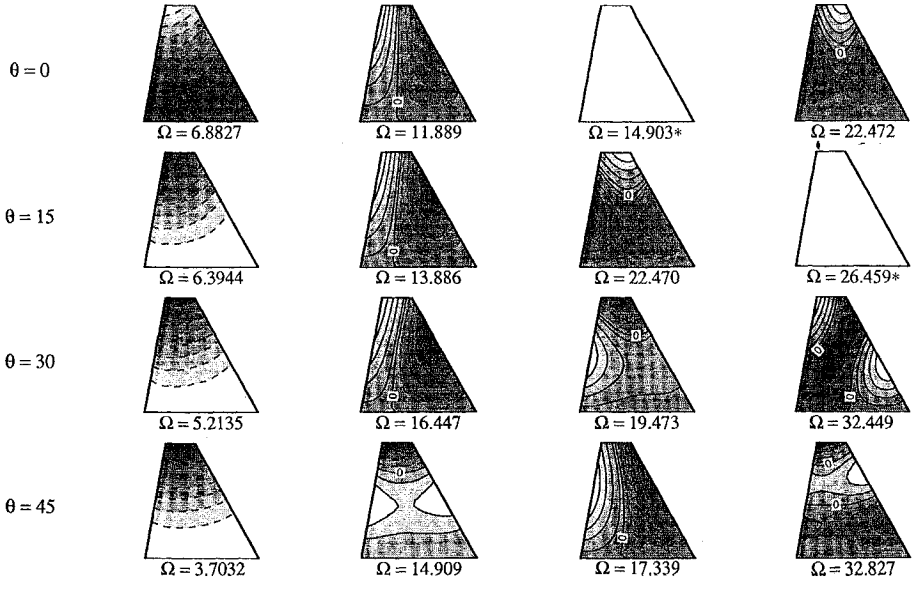

Fig. 5 Frequency parameters and mode shapes of cantilever, thick, skew, trapezoidal, symmetrically laminated $[-\theta/\theta/0]_s$ plates, $\Omega = \omega a^2/h)\sqrt{(\rho/E_2)}$, $\beta = 0$ deg, $q = 1.0$, $a/h = 10$, taper ratio = 0.25 (*in-plane mode).

The coefficients of the matrices in Eq. (21) are scaled values of the spring constants and are functions of x_i and y_i. Using the single dummy variable γ requires the additional restriction that $\mu = \upsilon$, or equivalently that $I = J = K = L = M = N = P = Q = R = S$.

Investigation of the convergence characteristics of the spring value, setting all values equal, leads to the appropriate choice,

$$\alpha_\xi = \beta_\xi = \{\max[(K_{\text{strain}})_{ij}]\} \times 10^7 \tag{23}$$

Equation (23) is an empirical relationship that was determined for the plates studied and is dependent upon the magnitude of the maximum value of the K_{strain} matrix. It is quite obvious that this magnitude is dependent upon the magnitudes of the material properties, the modulii and density, which are themselves dependent upon the units chosen. Thus, it may be desirable to derive an equation that takes into account the magnitude of the maximum K_{strain} value, but this has not been done in the present analysis since Eq. (23) is found for the plates investigated.

Table 9 Frequency parameter, $\Omega = (\omega a^2/h)\sqrt{(\rho/E_2)}$, for the first four frequencies of a cantilever, unsymmetrically laminated [−45/45], thick, skew, trapezoidal plate, with length-to-thickness ratio $a/h = 10$

q	Taper ratio	Sweep angle β, deg −45	−30	0	30	45
	0.25	2.92	2.65	2.52	3.60	4.91
		11.4	10.5	11.0	11.7	13.3
		12.6	14.6	12.7	17.6	19.8
		17.8	15.5	19.2	19.4	23.4
1.00	0.50	2.63	2.35	2.15	2.89	3.71
		9.81	8.95	9.46	9.12	10.2
		12.5	13.2	10.4	15.4	16.7
		15.5	14.1	17.2	16.7	19.5
	1.00	2.37	2.11	1.80	2.11	2.37
		7.02	6.05	5.86	6.05	7.02
		12.3	11.8	9.60	11.8	12.3
		13.1	13.0	14.6	13.0	13.1
	0.25	0.641	0.618	0.613	0.744	0.853
		3.02	2.88	2.87	3.40	3.88
		3.27	3.96	4.85	5.12	4.81
		7.29	6.62	6.13	6.78	7.83
2.00	0.50	0.564	0.537	0.518	0.607	0.681
		2.89	2.76	2.71	3.05	3.37
		3.26	3.82	4.44	4.51	4.19
		6.21	5.24	4.55	5.30	6.33
	1.00	0.509	0.472	0.430	0.472	0.509
		2.57	2.44	2.57	2.44	2.57
		3.48	3.61	2.76	3.61	3.48
		4.44	3.83	4.02	3.83	4.44
	0.25	0.0936	0.0917	0.0921	0.0989	0.104
		0.457	0.447	0.446	0.481	0.509
		0.824	1.03	1.05	1.04	0.872
		1.20	1.16	1.16	1.25	1.33
5.00	0.50	0.0801	0.0781	0.0775	0.0821	0.0861
		0.436	0.425	0.420	0.447	0.468
		0.707	0.950	0.987	0.982	0.766
		1.19	1.15	1.14	1.20	1.27
	1.00	0.0684	0.0661	0.0638	0.0661	0.0684
		0.422	0.410	0.399	0.410	0.422
		0.635	0.811	0.812	0.811	0.634
		1.18	1.15	1.07	1.15	1.18

A Fortran program was written for implementing the present method, with double-precision variables being employed throughout. The stiffness matrices and mass matrix were calculated numerically using eight-point Gaussian quadrature in both the η and ξ directions. Since the total stiffness and mass matrices are symmetric, and the mass matrix is positive definite, the IMSL subroutines DGVLRG and DGVCRG were used. DGVLRG gives only the eigenvalues, whereas DGVCRG gives both the eigenvalues and the associated eigenvectors. Where needed, the Chebychev polynomials and their derivatives are calculated as summations of lesser order Chebychev polynomials and derivatives, rather than explicitly through an algebraic expression. As described earlier, the same number of terms are taken in all of the series expansions shown in Eq. (4). A limitation in the implementation of the method is that the mass matrix no longer remains computationally positive definite when the number of terms in a given expansion series is greater than eight. Therefore, all results presented hereafter are for the 64-term displacement function series ($I = J = 8$) unless otherwise indicated, as in convergence studies. The resulting system has 320 degrees of freedom.

Results and Discussion

The present method has been applied to the free vibration of plates with various planforms, thicknesses, material composition, and boundary conditions. Excellent agreement is seen between the comparative references and the present approach.[7] The results for skew, trapezoidal, isotropic, thick, cantilever plates are presented in Table 1 for a length-to-thickness ratio of $b/h = 5$, $\gamma = 45$ deg, and $\upsilon = 0.3$. Comparison is made to McGee and Butalia[21] in the form of the frequency parameter $\Omega = \omega(a \cos \gamma)^2\sqrt{(\rho h/D)}$. The geometry and parameter definitions for these plates can be found in Ref. 21; however, it should be noted that γ is a trailing-edge sweep angle and D is the flexural rigidity. Excellent agreement is seen for these plates. Since the reference and present study allow for in-plane displacements, with Ref. 21 using the finite element method, in-plane modes are found by both methods.

Symmetrically laminated, thin, skew, trapezoidal, cantilever plates are presented in Table 2 for the lowest three frequencies, in hertz, for plates made from glass/epoxy. The properties for the glass/epoxy are $E_1 = 38.61$ GPa (5.6 Msi), $E_2 = E_3 = 8.27$ GPa (1.2 Msi), $G_{12} = G_{13} = 4.14$ GPa (0.6 Msi), $G_{23} = 3.35$ GPa, (0.49 Msi) (calculated letting $G_{23} = 0.81G_{12}$), $\upsilon_{12} = 0.26$, and $\rho = 2546.54$ kg/m^3 (4.94 slug/ft^3). The results are given for a plate with a sweep angle of $\beta = 30$ deg, aspect ratio = 3.111, taper ratio = 0.5, area = 406.45 cm^2 (63 in.^{2}), and a total

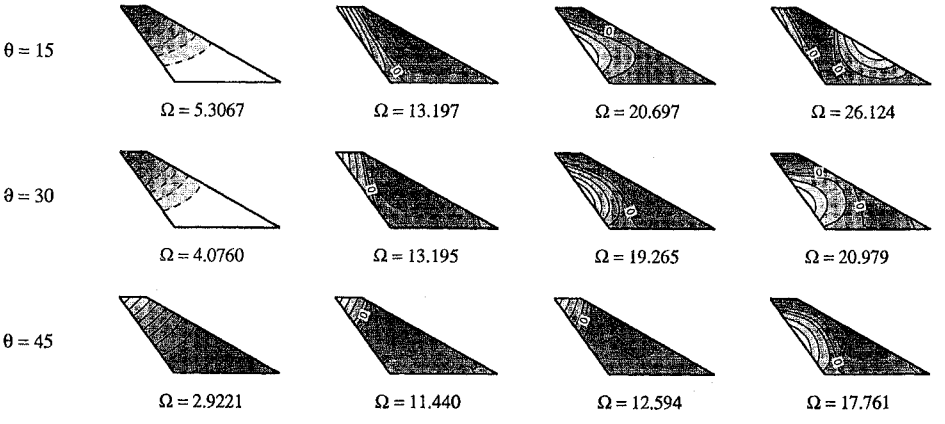

Fig. 6 Frequency parameters and mode shapes of cantilever, thick, skew, trapezoidal, unsymmetrically laminated $[-\theta/\theta]$ plates, $\Omega = (\omega a^2/h)\sqrt{(\rho/E_2)}$, $\beta = -45$ deg, $q = 1.0$, $a/h = 10$, taper ratio = 0.25.

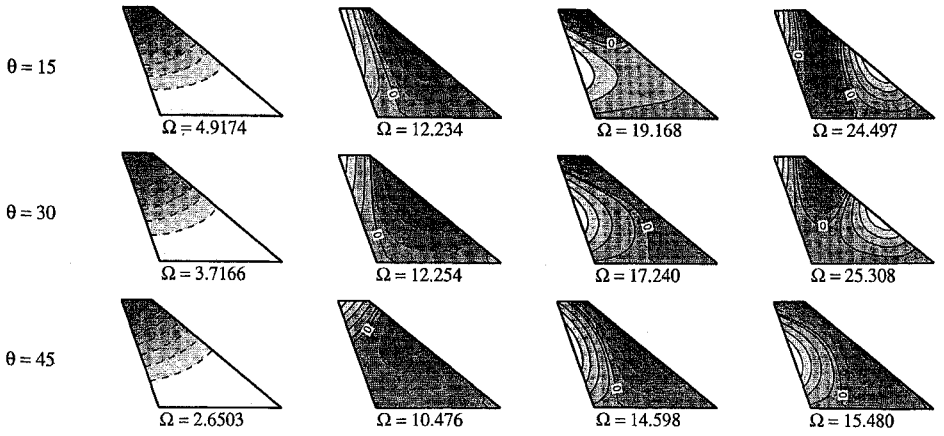

Fig. 7 Frequency parameters and mode shapes of cantilever, thick, skew, trapezoidal, unsymmetrically laminated $[-\theta/\theta]$ plates, $\Omega = (\omega a^2/h)\sqrt{(\rho/E_2)}$, $\beta = -30$ deg, $q = 1.0$, $a/h = 10$, taper ratio = 0.25.

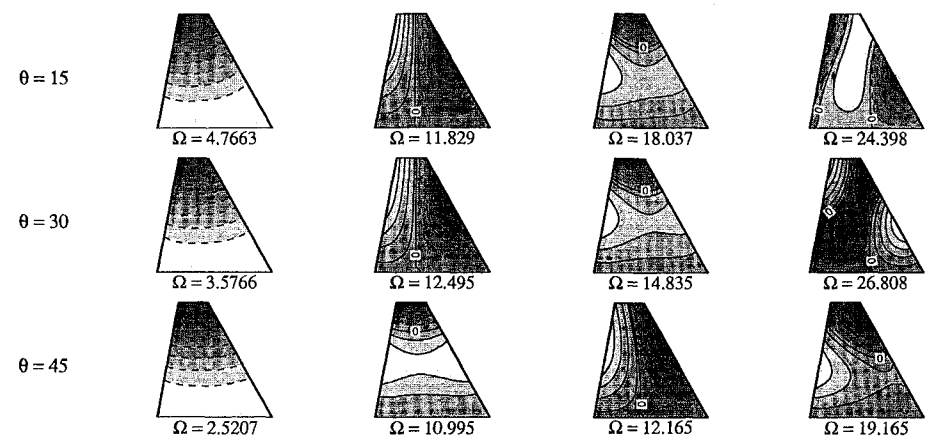

Fig. 8 Frequency parameters and mode shapes of cantilever, thick, skew, trapezoidal, unsymmetrically laminated $[-\theta/\theta]$ plates, $\Omega = (\omega a^2/h)\sqrt{(\rho/E_2)}$, $\beta = 0$ deg, $q = 1.0$, $a/h = 10$, taper ratio = 0.25.

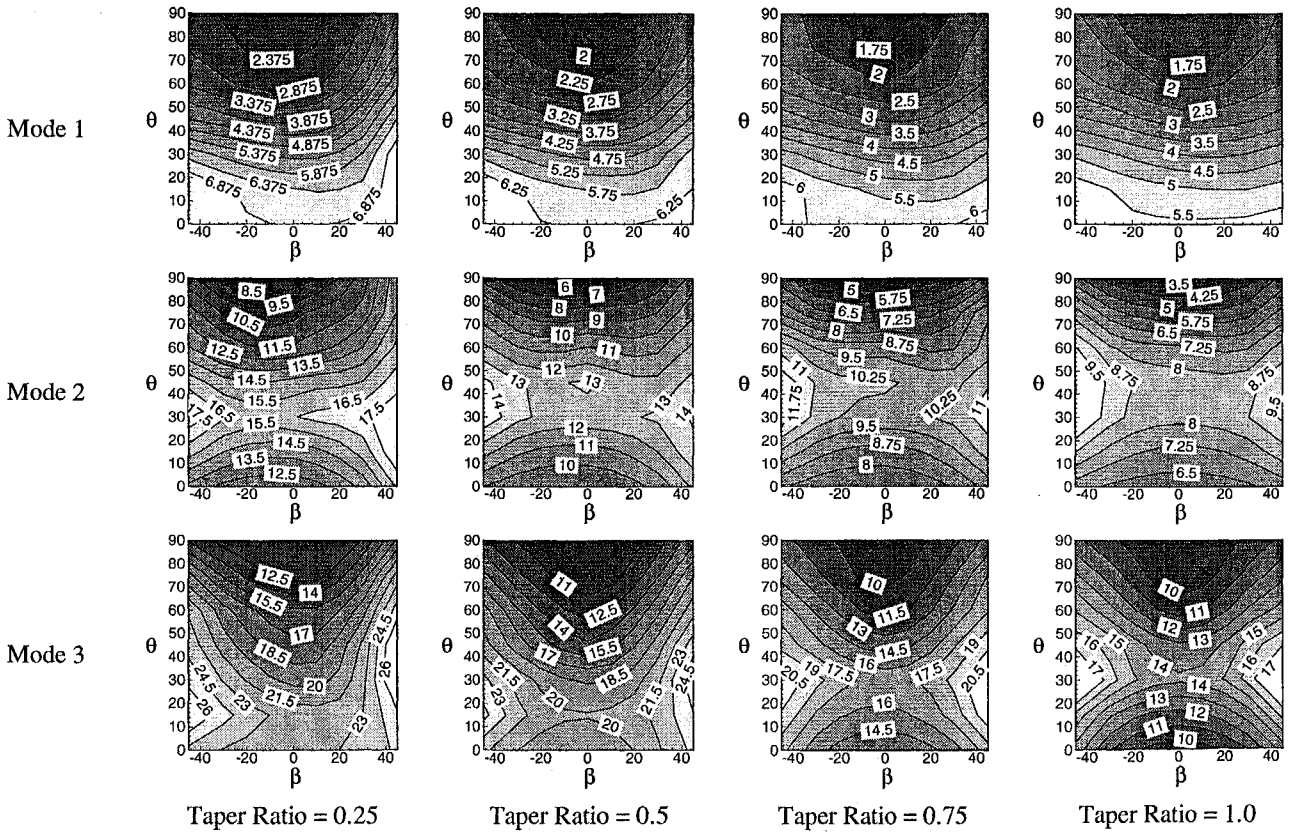

Fig. 9 Variation of frequency parameter, $\Omega = (\omega a^2/h)\sqrt{(\rho/E_2)}$, with respect to sweep angle in degrees, β, and fiber orientation angle θ, for the first three flexural modes of symmetrically laminated $[-\theta/\theta/0]_S$, thick, skew, trapezoidal, cantilever plates for $q = 1$ and $a/h = 10$.

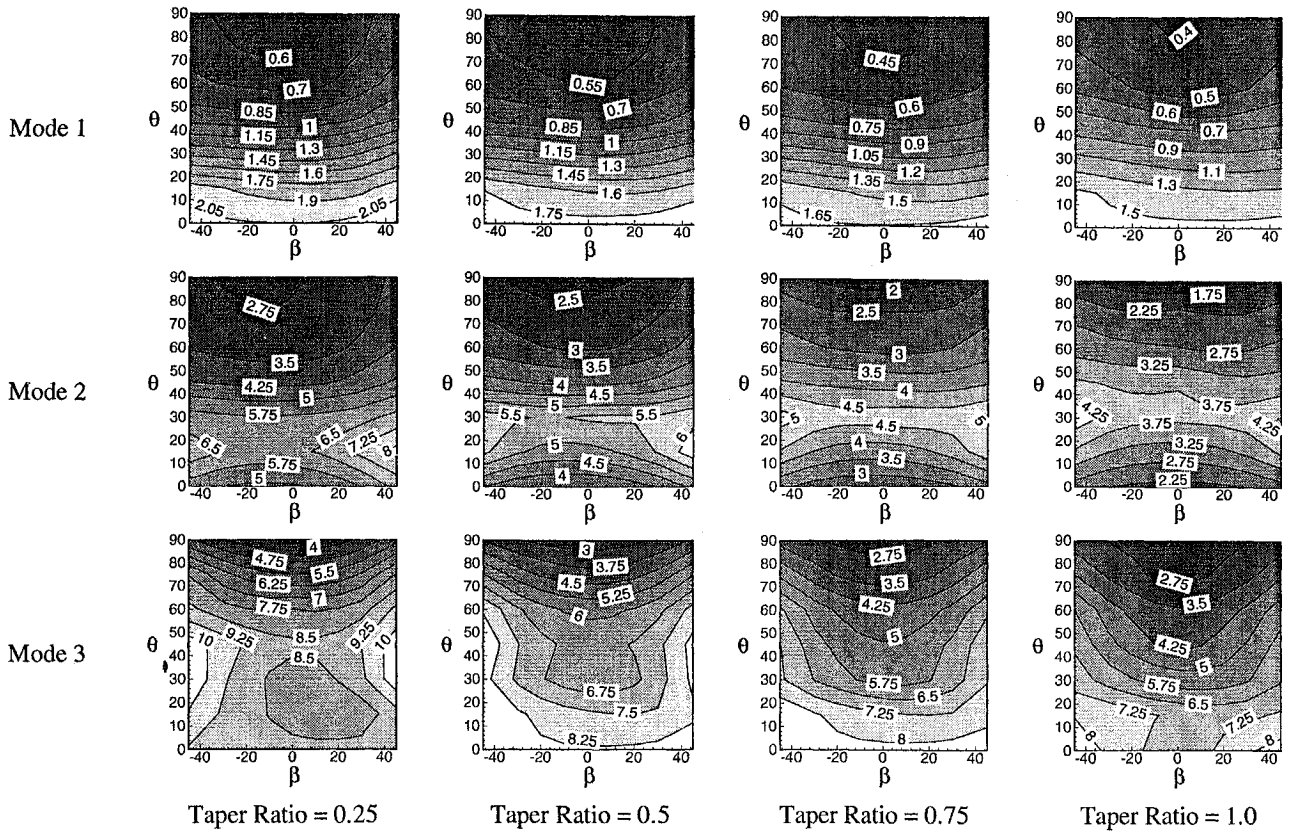

Fig. 10 Variation of frequency parameter, $\Omega = (\omega a^2/h)\sqrt{(\rho/E_2)}$, with respect to sweep angle in degrees, β, and fiber orientation angle θ, for the first three flexural modes of symmetrically laminated $[-\theta/\theta/0]_s$, thick, skew, trapezoidal, cantilever plates for $q = 2$ and $a/h = 10$.

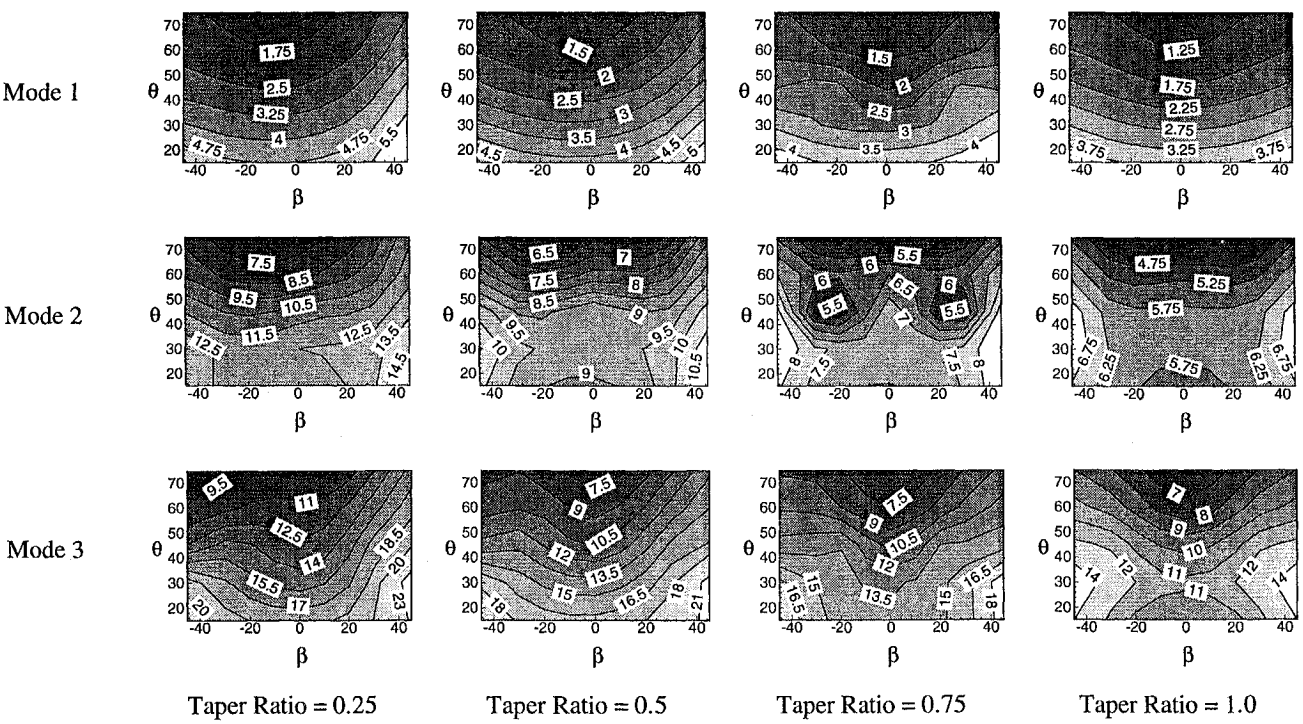

Fig. 11 Variation of frequency parameter, $\Omega = (\omega a^2/h)\sqrt{(\rho/E_2)}$, with respect to sweep angle in degrees, β, and fiber orientation angle θ, for the first three mode of unsymmetrically laminated $[-\theta/\theta]$, thick, skew, trapezoidal, cantilever plates for $q = 1$ and $a/h = 10$.

thickness of 3.556 mm (0.14 in.) for various values of θ within the stacking sequence $[\theta_2/0]_s$. Both Lakshminarayana et al.[24] and Lee and Lee[25] present results based on FSDT finite elements, but neither reference gives results for thick, skew, trapezoidal, laminated plates. Additionally, for the results presented in Table 2, Lee and Lee[25] give the aspect ratio incorrectly as 2.333. Very good agreement is seen between the present method and the references. Table 3 gives results for $[-30/30/0]_s$ plates of the same material and a variety of geometries.

Unsymmetrically laminated [0/22.5], boron/epoxy, skew, trapezoidal plate results are compared with those of Kapania and Singhvi[16] in Table 4. The plate area is 412.9 cm^2 (64 in.^{2}), with a total thickness of 1.2497 mm (0.0492 in.) and a taper ratio of 0.75. The plates are constructed of boron/epoxy having properties of

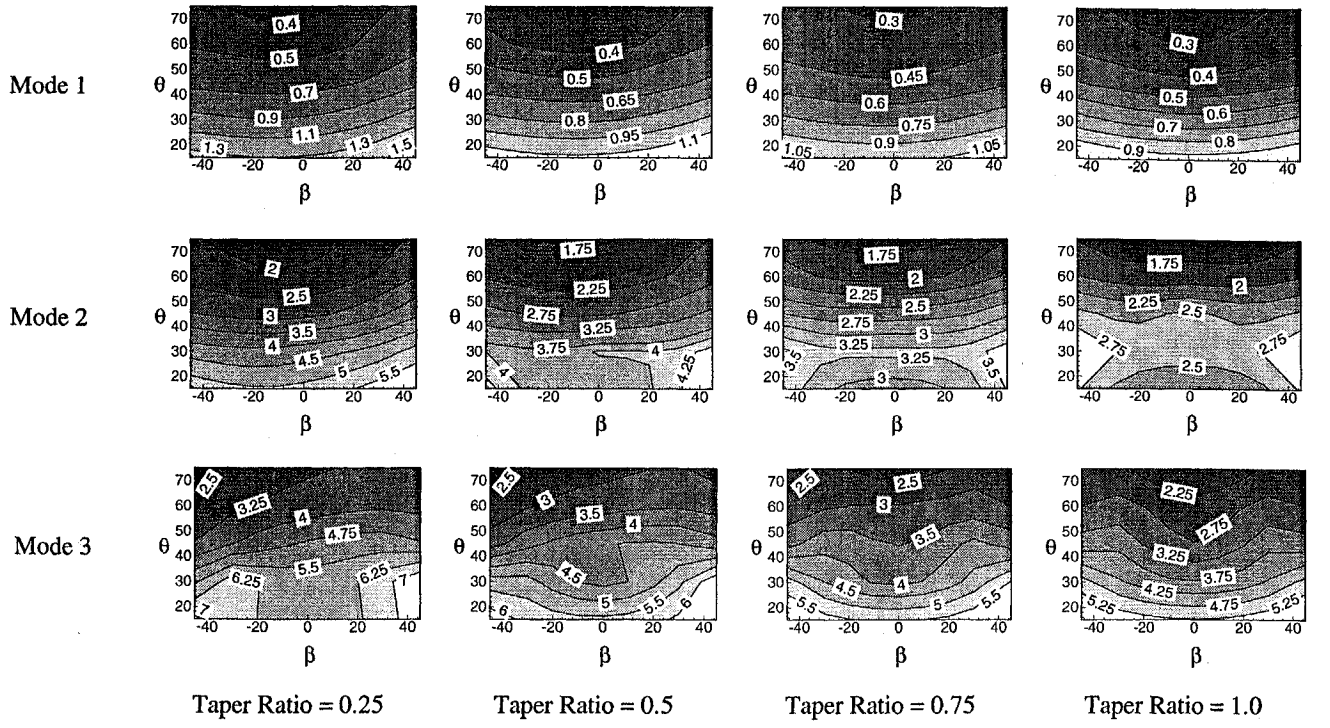

Fig. 12 Variation of frequency parameter, $\Omega = (\omega a^2/h)\sqrt{(\rho/E_2)}$, with respect to sweep angle in degrees, β, and fiber orientation angle θ, for the first three modes of unsymmetrically laminated $[-\theta/\theta]$, thick, skew, trapezoidal, cantilever plates for $q = 2$ and $a/h = 10$.

$E_1 = 161.21$ GPa (23.38 Msi), $E_2 = E_3 = 12.52$ GPa (1.82 Msi), $G_{12} = G_{13} = 6.75$ GPa (0.98 Msi), $G_{23} = 5.47$ GPa (0.79 Msi) (calculated as before), $\upsilon_{12} = 0.22$, and $\rho = 1881.81$ kg/m^3 (3.65 slug/ft^3). Frequencies, in hertz, are given for ranges of aspect ratio and sweep angle. Since transverse shear can have a significant effect for unsymmetrically laminated plates, even if they are thin, it is expected that the present method should give noticeably lower frequencies. With the exception of the fifth frequency for the plate of aspect ratio of 5 and sweep angle of 45 deg, this is indeed the case.

To present some insight into the free vibration behavior of thick, generally laminated, skew, trapezoidal, cantilever plates, an extensive study has been conducted. The plate geometry is changed by varying the values of the quarter-chord multiplier q, the taper ratio, and the sweep angle β. In addition, for symmetrically laminated $[-\theta/\theta/0]_s$ and unsymmetrically laminated $[-\theta/\theta]$ plates, values for θ of 15, 30, 45, 60, and 75 deg are considered. For the symmetrically laminated plates, values for θ of 0 and 90 deg are also considered. The plates are composed of a material with the following properties: $E_1/E_2 = 40$, $G_{12}/E_2 = G_{13}/E_2 = 0.6$, $G_{23}/E_2 = 0.5$, and $\upsilon_{12} = 0.25$. Results are given using the frequency parameter $\Omega = (\omega a^2/h)\sqrt{(\rho/E_2)}$, with a length-to-thickness ratio $a/h = 10$. A representative convergence plot for the stacking sequence $[-30/30/0]_s$, with $\beta = -45$ deg and taper ratio $= 0.25$, is given in Fig. 2, where it is seen that convergence of the solutions is satisfactory. Similar results are obtained for the other plates studied.

In the Ref. 7, sweep angles were studied using values of $\beta = -45, -30, -20, -10, 0, 10, 20, 30$, and 45 deg. Values for the q parameter were chosen as 1, 2, and 5. Tables 5–9 give some representative results for these plates. Some representative mode shape plots are given in Figs. 3–5 for symmetrically laminated and in Figs. 6–8 for unsymmetrically laminated plates. The plates are clamped along the bottom edge in the figures, and the nodal lines are indicated by the various 0.

Using the tabulated data, representative contour plots of the frequency parameter behavior, as a function of sweep angle and fiber orientation angle, have been made and are presented in Figs. 9–12. For all thick, laminated, skew, trapezoidal, cantilever plates studied, it is seen that the frequencies decrease as the value for the parameter q increases. Also, with an increase in taper ratio, the frequencies decrease. Additionally, for such contour plots, an optimum θ can be found for a particular plate geometry.

Summary and Conclusions

An approximate approach has been developed to analyze the natural frequencies of generally laminated, thick, skew, trapezoidal plates with various edge supports. In this method, Chebychev polynomials are used as trial functions in the Rayleigh–Ritz method as applied to an FSDT formulation. Although the present method is applicable to any edge-supported plate, in the current study, skew, trapezoidal, cantilever plates are compared with published results when possible, and results for thick plates are presented. Since laminated plate vibrations are dependent upon a great number of variables, including angular stacking sequence and material stacking sequence, the frequency parameters presented are not as useful in design as those for isotropic plates. It is not the intent of this study to present design information but to make available data for comparative purposes with other methods, data that are not available at this time in the literature. Lastly, since this simple approach yields accurate results for a large variety of plates without the necessity of choosing functions that satisfy the essential boundary conditions,[7] it can be easily implemented for design or optimization calculations.

The collection of results, representing a large variation of planforms for both symmetrically and unsymmetrically laminated, thick, skew, trapezoidal, cantilever plates clearly show some general qualitative trends for the frequency. They are as follows: 1) as the value of q, a measure of span, increases, the frequency decreases; 2) as the sweep angle β moves away from 0 deg in either the positive or negative direction, the frequency generally tends to increase; 3) as the taper ratio increases, the frequency decreases; 4) for bending modes, the value of the frequency decreases as the fiber orientation angle θ moves away from 0; and 5) for torsional modes, the value of the frequency as a function of the fiber orientation angle θ is dependent upon the geometric parameters.

References

[1]Jones, R. M., *Mechanics of Composite Materials*, Hemisphere, New York, 1975.

[2]Vinson, J. R., and Sierakowski, R. L., *The Behavior of Structures Composed of Composite Materials*, Kluwer Academic, Dordrecht, The Netherlands, 1987.

[3]Whitney, J. M., *Structural Analysis of Laminated Anisotropic Plates*, Technomic, Lancaster, PA, 1987.

[4]Reddy, J. N., "A General Non-Linear Third-Order Theory of Plates with Moderate Thickness," *International Journal of Non-Linear Mechanics*, Vol. 25, No. 6, 1990, pp. 677–686.

[5]Reddy, J. N., "A Simple Higher-Order Theory for Laminated Composite Plates," *Journal of Applied Mechanics*, Vol. 51, No. 4, 1984, pp. 745–752.

[6]Robbins, D. H., Jr., and Reddy, J. N., "Modeling of Thick Composites Using a Layerwise Laminate Theory," *International Journal for Numerical Methods in Engineering*, Vol. 36, No. 4, 1993, pp. 655–677.

[7]Lovejoy, A. E., and Kapania, R. K., "Natural Frequencies and an Atlas of Mode Shapes for Generally-Laminated, Thick, Skew, Trapezoidal Plates," Center for Composite Materials and Structures, Virginia Polytechnic Inst. and State Univ., Rept. 94-09, Blacksburg, VA, Aug. 1994.

[8]Chia, C.-Y., "Geometrically Nonlinear Behavior of Composite Plates: A Review," *Applied Mechanics Review*, Vol. 41, No. 12, 1988, pp. 439–451.

[9]Kapania, R. K., and Raciti, S., "Recent Advances in Analysis of Laminated Beams and Plates, Part I: Shear Effects and Buckling," *AIAA Journal*, Vol. 27, No. 7, 1989, pp. 923–934.

[10]Kapania, R. K., and Raciti, S., "Recent Advances in Analysis of Laminated Beams and Plates, Part II: Vibrations and Wave Propagation," *AIAA Journal*, Vol. 27, No. 7, 1989, pp. 935–946.

[11]Leissa, A. W., "Advances in Vibration, Buckling and Postbuckling Studies on Composite Plates," *Composite Structures (Proceedings of the 1st International Conference, 1981)*, edited by I. H. Marshal, Science Publishers, London, 1981, pp. 312–334.

[12]Reddy, J. N., "On Refined Theories of Composite Laminates," *Meccanica*, Vol. 25, No. 4, 1990, pp. 230–238.

[13]Reddy, J. N., "Finite Element Modeling of Structural Vibrations: A Review of Recent Advances," *Shock and Vibration Digest*, Vol. 11, No. 1, 1979, pp. 25–39.

[14]Reddy, J. N., "A Review of the Literature on Finite-Element Modeling of Laminated Composite Plates," *Shock and Vibration Digest*, Vol. 17, No. 4, 1985, pp. 3–8.

[15]Reddy, J. N., "A Review of Refined Theories of Laminated Composite Plates," *Shock and Vibration Digest*, Vol. 22, No. 7, 1990, pp. 3–17.

[16]Kapania, R. K., and Singhvi, S., "Free Vibration Analysis of Generally Laminated Tapered Skew Plates," *Composite Engineering*, Vol. 2, No. 3, 1992, pp. 197–212.

[17]Srinivasan, R. S., and Babu, B. J. C., "Free Vibration of Cantilever Quadrilateral Plates," *Journal of the Acoustical Society of America*, Vol. 73, No. 3, 1983, pp. 851–855.

[18]Joshi, A., and Madhusudhan, B. S., "Sensitivity of Free Vibration Characteristics of Cantilever Plates to Geometric Parameters," *Journal of Sound and Vibration*, Vol. 145, No. 3, 1991, pp. 489–494.

[19]Laura, P. A. A., Gutierrez, R. H., and Bhat, R. B., "Transverse Vibrations of a Trapezoidal Cantilever Plate of Variable Thickness," *AIAA Journal*, Vol. 27, No. 7, 1989, pp. 921, 922.

[20]McGee, O. G., Leissa, A. W., and Huang, C. S., "Vibrations of Cantilevered Skewed Trapezoidal and Triangular Plates with Corner Stress Singularities," *International Journal of Mechanical Sciences*, Vol. 34, No. 1, 1992, pp. 63–84.

[21]McGee, O. G., and Butalia, T. S., "Natural Vibrations of Shear Deformable Cantilevered Skewed Trapezoidal and Triangular Thick Plates," *Computers and Structures*, Vol. 45, No. 5/6, 1992, pp. 1033–1059.

[22]Liew, K. M., and Lam, K. Y., "A Rayleigh-Ritz Approach to Transverse Vibration of Isotropic and Anisotropic Trapezoidal Plates Using Orthogonal Plate Functions," *International Journal of Solids and Structures*, Vol. 27, No. 2, 1991, pp. 189–203.

[23]Krishnan, A., and Deshpande, J. V., "A Study on Free Vibration of Trapezoidal Plates," *Journal of Sound and Vibration*, Vol. 146, No. 3, 1991, pp. 507–515.

[24]Lakshminarayana, H. V., Rajagopal, P., Ramamurthy, M. R., and Joshi, A., "Vibration Characteristics of a Swept Composite Wing Panel: Finite Element Analysis and Experimental Verification," *Journal of the Aeronautical the Society of India*, Vol. 37, No. 4, 1985, pp. 289–295.

[25]Lee, I., and Lee, J. J., "Vibration Analysis of Composite Plate Wing," *Computers and Structures*, Vol. 37, No. 6, 1990, pp. 1077–1085.

[26]Cook, R. D., Malkus, D. S., and Plesha, M. E., *Concepts and Applications of Finite Element Analysis*, 3rd ed., Wiley, New York, 1989.

[27]Cederbaum, G., Librescu, L., and Elishakoff, I., "Remarks on a Dynamic Higher-Order Theory of Laminated Plates and Its Application in Random Vibration Response," *International Journal of Solids and Structures*, Vol. 25, No. 5, 1989, pp. 515–526.

[28]Mindlin, R. D., "Influence of Rotatory Inertia and Shear on Flexural Motions of Isotropic, Elastic Plates," *Journal of Applied Mechanics*, Vol. 18, No. 1, 1951, pp. 31–38.

[29]Chatterjee, S. N., and Kulkarni, S. V., "Shear Correction Factors for Laminated Plates," *AIAA Journal*, Vol. 17, No. 5, 1979, pp. 498, 499.

[30]Chou, P. C., and Carleone, J., "Transverse Shear in Laminated Plate Theories," *AIAA Journal*, Vol. 11, No. 9, 1973, pp. 1333–1336.

[31]Chow, T. S., "On the Propagation of Flexural Waves in an Orthotropic Laminated Plate and Its Response to an Impulsive Load," *Journal of Composite Materials*, Vol. 5, July 1971, pp. 306–319.

[32]Kam, T. Y., and Chang, R. R., "Buckling of Shear Deformable Laminated Composite Plates," *Composite Structures*, Vol. 22, No. 4, 1992, pp. 223–234.

[33]Whitney, J. M., "Shear Correction Factors for Orthotropic Laminates Under Static Loading," *Journal of Applied Mechanics*, Vol. 40, No. 1, 1973, pp. 302–304.

[34]Whitney, J. M., "Stress Analysis of Thick Laminated Composite and Sandwich Plates," *Journal of Composite Materials*, Vol. 6, Oct. 1972, pp. 426–440.

[35]Whitney, J. M., and Sun, C. T., "A Higher Order Theory for Extensional Motion of Laminated Composites," *Journal of Sound and Vibration*, Vol. 30, No. 1, 1973, pp. 85–97.

[36]Reddy, J. N., and Chao, W. C., "Non-Linear Bending of Thick Rectangular, Laminated Composite Plates," *International Journal of Non-Linear Mechanics*, Vol. 16, No. 3/4, 1981, pp. 291–301.